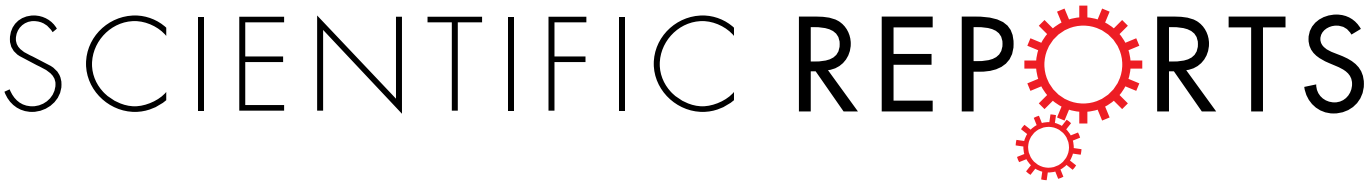

OPEN

Weakly-coupled quasi-1D helical modes in disordered 3D topological insulator quantum wires

Received: 22 September 2016
Accepted: 23 February 2017
Published: 04 April 2017

J. Dufouleur[1,*], L. Veyrat[1,*], B. Dassonneville[1], E. Xypakis[2], J. H. Bardarson[2], C. Nowka[1], S. Hampel[1], J. Schumann[1], B. Eichler[1], O. G. Schmidt[1], B. Büchner[1,3] & R. Giraud[1,4]

Disorder remains a key limitation in the search for robust signatures of topological superconductivity in condensed matter. Whereas clean semiconducting quantum wires gave promising results discussed in terms of Majorana bound states, disorder makes the interpretation more complex. Quantum wires of 3D topological insulators offer a serious alternative due to their perfectly-transmitted mode. An important aspect to consider is the mixing of quasi-1D surface modes due to the strong degree of disorder typical for such materials. Here, we reveal that the energy broadening γ of such modes is much smaller than their energy spacing Δ, an unusual result for highly-disordered mesoscopic nanostructures. This is evidenced by non-universal conductance fluctuations in highly-doped and disordered Bi2Se3 and Bi_2Te_3 nanowires. Theory shows that such a unique behavior is specific to spin-helical Dirac fermions with strong quantum confinement, which retain ballistic properties over an unusually large energy scale due to their spin texture. Our result confirms their potential to investigate topological superconductivity without ambiguity despite strong disorder.

In a quantum wire of a strong 3D topological insulator (3DTI), the confinement of spin-helical Dirac fermions modifies the energy distribution of topological surface states in the transverse direction. Quasi-1D propagating surface modes form (see Fig. 1), and their transverse energy is quantized with an energy level spacing $\Delta = h v_F/L_p$ that is directly related to the perimeter L_p of the nanostructure. In zero magnetic field, their energy spectrum is obtained from the intersection of the spin-textured Dirac cone with equally-spaced quantized planes, separated by $\delta k_\perp = 2\pi/L_p$. A gap opens at the Dirac point and pairs of degenerate modes loose their topological protection. In presence of disorder, quantized modes are mixed and their transverse energy broadens over an energy scale Γ (see Fig. 1b). Besides, their energy spectrum can be tuned by applying a magnetic field $B_{||}$ along the length of the nanowire[1]. Cyclic boundary conditions are changed and the additional phase introduced by the circulation of the vector potential along the perimeter, equivalent to a change in the transverse impulse, induces an overall energy shift of all modes. Importantly, a single gapless transverse mode with perfect transmission develops by tuning the magnetic flux $\Phi = B_{||} \times S$ to half of a flux quantum $\Phi_0 = h/e$, S being the electrical cross section of the wire, and it is topologically protected[1–4]. This evolution between an even or an odd number of quantized modes is periodic in flux, with a period Φ_0.

By proximity with a superconducting contact, this perfectly-transmitted mode induces topological superconductivity in the quantum wire and Majorana bound states are predicted to form at the S/TI interface[5–7]. A remarkable property is the robustness against non-magnetic disorder, in contrast to other systems hosting topological superconductivity[8,9]. In clean semiconducting nanowires, the interpretation of tunnel spectroscopy based on Majorana states[10–12] is made complex by disorder[13–20]. In dirty 3DTI quantum wires, the influence of disorder is reduced and, interestingly, the nature of superconductivity could be tuned with the magnetic flux. Besides, the signature of Majorana states should appear in both the interface resistance of S/TI junctions[7] and the current-phase relation of the supercurrent in Josephson junctions[21]. Although the experimental setup is rather simple, two important conditions must be satisfied so as to evidence zero-energy quasi-particles. First, the chemical potential must be tuned close to the Dirac point. This remains a challenge for all known 3D TI quantum

[1]Leibniz Institute for Solid State and Materials Research, IFW Dresden, D-01069 Dresden, Germany. [2]Max-Planck-Institut für Physik Komplexer Systeme, Nöthnitzer Straße 38, D-01187 Dresden, Germany. [3]Department of Physics, TU Dresden, D-01062 Dresden, Germany. [4]INAC-SPINTEC, Univ. Grenoble Alpes/CNRS/CEA, 17 Avenue des Martyrs, F-38054 Grenoble, France. *These authors contributed equally to this work. Correspondence and requests for materials should be addressed to R.G. (email: r.giraud@ifw-dresden.de)

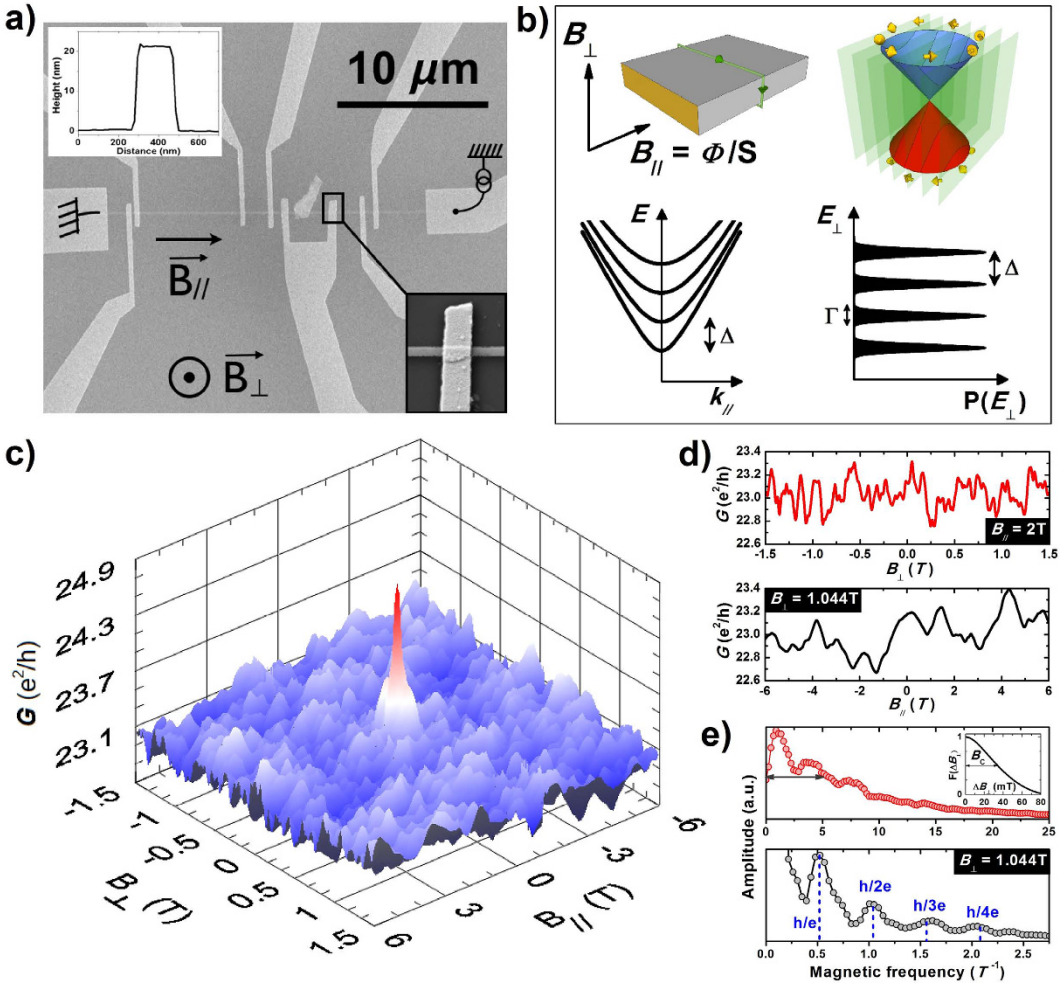

Figure 1. Quantum corrections to the classical conductance of a short-perimeter Bi_2Se_3 quantum wire. (**a**) Scanning electron microscope image of a narrow Bi_2Se_3 nanoribbon (width $w = 170$ nm, height $h = 20$ nm and perimeter $L_p = 380$ nm), contacted with CrAuAl leads. Three mesoscopic conductors are measured, with different lengths $L_1 \approx 400$ nm, $L_2 \approx 1\,\mu$m and $L_3 \approx 6\,\mu$m. Inset: Profile of the atomically flat structure measured by atomic force microscopy. (**b**) Schematics of the measurement geometry in magnetic field and of the quasi-1D energy modes induced by quantum confinement, with a transverse energy spacing Δ. Disorder leads to mode mixing, which results in the broadening Γ of quantized modes. (**c**) Longitudinal and transverse magneto-conductance $G(B_{||}, B_\perp)$ of the quantum wire with length $L_2 = 1\,\mu$m, for which $l_{tr} \approx L_p < L_2 < L_\varphi$, measured at $T = 30$ mK. (**d**) Details from (**c**): *top*, $G(B_\perp)$ for a constant $B_{||} = 2$ T (aperiodic conductance fluctuations), and *bottom*, $G(B_{||})$ for a constant $B_\perp = 1.044$ T (periodic Aharonov-Bohm oscillations). (**e**) Fast-Fourier transforms of magneto-conductance traces shown in (**d**). For conductance fluctuations (top), a small non-monotonous background is intrinsic to the limited field range studied and only the half-width at half-maximum (horizontal arrow) has a physical meaning (it corresponds to the 200 mT quasi-period seen in d). The overall damping over 25 T^{-1} relates to the 30 mT correlation field inferred from the correlation function $F(\Delta B_\perp) = \langle G(B_\perp)G(B_\perp + \Delta B_\perp)\rangle$ shown in inset. For Aharonov-Bohm oscillations (bottom), four harmonics clearly arise from the background (vertical dashed lines).

wires, which are often strongly doped due to structural disorder. Charge compensation with extrinsic impurities is required, which increases the degree of disorder. Second, the broadening Γ of quantized transverse energies should remain smaller than their spacing Δ, a condition which is not obvious to realize in highly-disordered quantum wires. Here, we reveal that 3D TI nanostructures do satisfy the condition $\Gamma < \Delta$ despite strong disorder, due to the weak scattering of spin-helical modes, contrary to the case of metallic or semiconducting nanowires, for which the mixing of quantized modes by disorder is always efficient. This is unambiguously evidenced by disorder-sensitive quantum coherent transport experiments, which further give important information about the nature of surface charge transport. We report on the first observation of non-universal conductance fluctuations in a highly-disordered mesoscopic conductor, and show that the unusual transport properties of quasi-1D surface modes in 3D TI quantum wires are due to their spin structure.

In a mesoscopic wire, when the phase coherence length $L_\varphi(T)$ of quasi-particles becomes comparable to the length L of a conductor, quantum interference modifies the conductance. For a 3D TI quantum wire, the different

quantum corrections to the conductance due to topological surface states can be separated, depending on the orientation of the applied magnetic field (see Supplementary Informations:sections I & III-B). Applying the field $B_{||}$ parallel to the length of a nanostructure induces a well-defined Aharonov-Bohm phase and periodic oscillations of the conductance are induced by the magnetic flux $\Phi = B_{||} \times S$[1]. These were evidenced in Bi_2Se_3 nanostructures[22], and a study of decoherence at very low temperature revealed the quasi-ballistic nature of charge transport in short-perimeter nanowires[23]. Applying a transverse magnetic field $B_{\perp}$, disorder results in aperiodic conductance fluctuations, and their statistical properties depend on the nature and the dimensionality of the transport regime[24]. Whereas conductance fluctuations are sample-specific in ballistic conductors, provided that the classical dynamics of the conductor is not chaotic[25,26], a small amount of impurities usually drives a system into the diffusive regime, for which conductance fluctuations are universal. In most cases, the ballistic-diffusive transition is rather abrupt since momentum scattering is strong enough that diffusive transport already occurs for a conductor length $L \gtrsim l_e$, where l_e is the elastic mean free path, so that conductance fluctuations are usually universal in mesoscopic conductors[27–29]. In rare cases, for which momentum scattering is weak, this transition is smoother since it happens for $L \gtrsim l_{tr} \gg l_e$, where the transport length l_{tr}, typical of backscattered trajectories, becomes the relevant length scale for diffusive transport[24]. Such a situation happens for spin-helical Dirac fermions in a 3D topological insulator due to the spin-momentum locking, which results in enhanced forward scattering and therefore in a transport mean free path l_{tr} much longer than the elastic mean free path l_e[30,31]. If a mesoscopic conductor is set within the ballistic-to-diffusive crossover, non-universal conductance fluctuations can be observed, and their statistical properties strongly depend on details of the quasi-particles' energy spectrum and on their interplay with disorder, as shown below.

Results

To investigate the nature of the *longitudinal* motion of helical Dirac fermions and the broadening of quantized surface modes by disorder, we study the conductance fluctuations of long mesoscopic 3D TI quantum wires in the limit $L \geq l_{tr}$, for which diffusive transport along the nanowire is expected. The Thouless energy remains smaller than the energy level spacing, in the sub-meV range. For clarity, we discuss below the results obtained in two different limits. First, large non-universal conductance fluctuations are evidenced in short-perimeter Bi_2Se_3 quantum wires (strong quantum confinement). In this limit $L_\varphi \gg L_p$, the periodic behavior of Aharonov-Bohm oscillations is not directly seen in magneto-conductance traces, due to their multiple-harmonic nature and disorder, but it can be revealed by a Fourier-transform analysis[23]. Due to the large energy level spacing Δ (reduced number of transverse modes), the non-universal behavior of conductance fluctuations is best observed. Second, smaller but clear non-universal conductance fluctuations are evidenced in long-perimeter Bi_2Te_3 quantum wires (small quantum confinement). In this limit $L_\varphi \gtrsim L_p$, the periodic behavior of Aharonov-Bohm oscillations is directly seen in magneto-conductance traces (fundamental harmonic). Similar conclusions on the non-universal behavior of conductance fluctuations can be drawn, thus confirming their origin from surface mode transport, as well as the robust energy dependence of quasi-ballistic properties for all spin-helical modes.

Experiments

Using a 3D-vector superconducting magnet, the quantum corrections to the classical conductance of mesoscopic 3D TI quantum wires were measured by controlling the longitudinal and transverse magnetic fields independently. For a complete $G(B_{||}, B_{\perp})$ mapping, the magnetic flux was set to a well-defined value (constant value of $B_{||}$) and magneto-conductance traces $G(B_{\perp})$ were measured. Importantly, the transverse magnetic field has little influence on the high-energy spectrum of confined Dirac fermions and it can therefore be conveniently used to probe aperiodic conductance fluctuations due to surface states, independently from Aharonov-Bohm conductance oscillations. See Supplementary Informations:sections I & II for details.

Short-perimeter quantum wires. The largest amplitude of non-universal conductance fluctuations is revealed in short-perimeter Bi_2Se_3 quantum wires, with a perimeter $L_p = 380$ nm. Due to a high density of Se vacancies acting as donors, these nanostructures are metallic, with the surface Fermi energy E_F lying about 250 meV above the Dirac point. The total conductance results from a comparable contribution from surface and bulk carriers, as inferred from classical magneto-resistance and transconductance measurements on wide nanoribbons[31,32], but conductance fluctuations in long wires are dominated by topological surface states, as shown below (see also Supplementary Informations: I). For helical Dirac fermions in the narrow Bi_2Se_3 wires considered here, the energy level spacing $\Delta \approx 6$ meV gives $N \approx 2E_F/\Delta \approx 80$ transverse modes, and we find $l_{tr} < 300$ nm, using $v_F \approx 5 \cdot 10^5$ ms^{-1} obtained from angle-resolved photoemission spectroscopy[33–35] (see Supplementary Informations: II-D).

An example of the full mapping of quantum corrections to the classical conductance, measured at $T = 30$ mK, is shown in Fig. 1c) for a wire length $L_2 = 1\ \mu$m. Quantum interference of topological surface states results in a sharp weak anti-localization peak around zero field and in a different field dependence of the conductance depending on whether the magnetic field is swept along the wire axis (slow Aharonov-Bohm oscillations) or perpendicular to it (fast aperiodic fluctuations), as seen in Fig. 1d). The distinct nature of quantum interference patterns in finite field is clearly evidenced by the Fourier transform of the magneto-conductance traces measured in either a longitudinal or a perpendicular field (Fig. 1e), revealing their periodic or aperiodic characteristics, respectively, and their very different correlation fields. To investigate the nature of conductance fluctuations, the standard deviation δG_{rms} is evaluated from $B_{\perp}$ sweeps over a 3T range, which is much larger than the correlation field $B_C \approx 30$ mT inferred from the correlation function $\langle G(B)G(B+\Delta B)\rangle$ (see inset in Fig. 1e), for constant values of the magnetic flux ($B_{||}$ is fixed). At low-enough temperatures, when $L_\varphi(T) \geq L$, δG_{rms} saturates at a value δG_{rms}^{sat}, as known for a mesoscopic conductor in the fully-coherent regime. However, this value varies with the longitudinal magnetic field (Fig. 2a) instead of being fixed to a universal value, as expected for diffusive transport ($L_\varphi \geq L \geq l_{tr}$) in general and for highly-disordered topological insulators without quantum confinement in

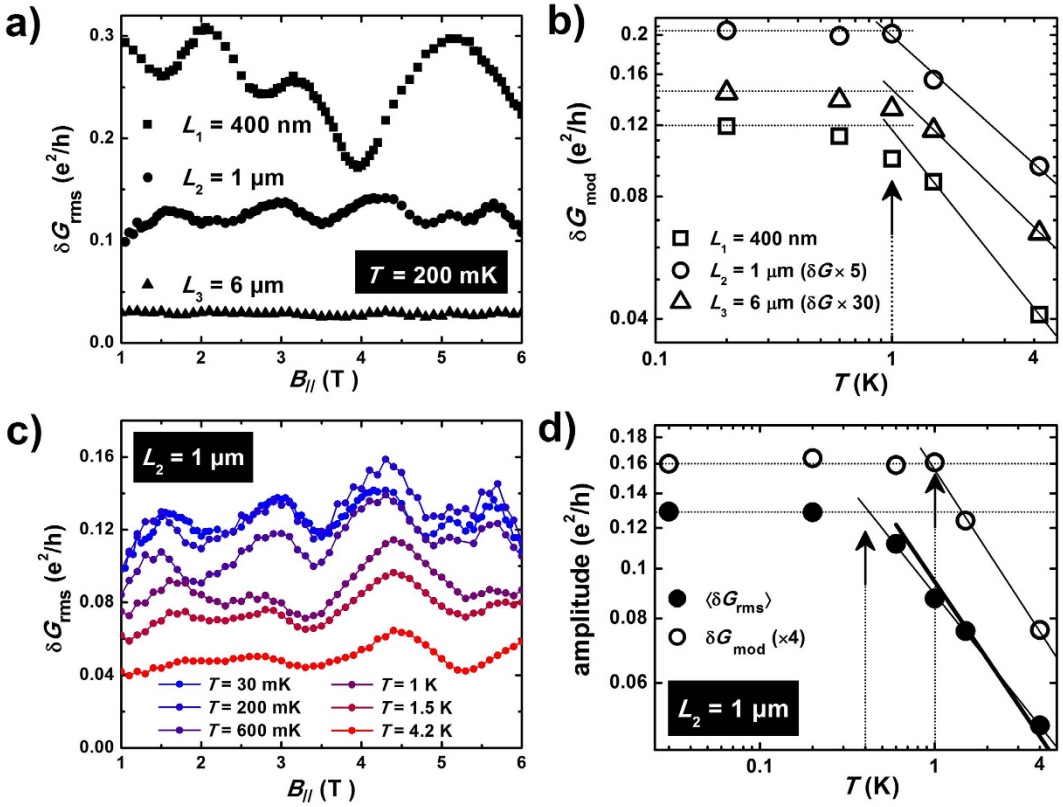

Figure 2. Non-universal conductance fluctuations modulated by the longitudinal field. (**a**) Longitudinal-field dependence of the standard deviation of conductance fluctuations δG_{rms} measured at $T = 200$ mK for three different lengths, with $l_{tr} \approx L_1 < L_\varphi$, $l_{tr} < L_2 \approx L_\varphi$ and $l_{tr} < L_\varphi < L_3$. For a given value of the magnetic flux, δG_{rms} is evaluated from $B_\perp$ sweeps over a 3T range, with no need of a background substraction (negligible classical magneto-resistance). Non-universal conductance fluctuations due to surface modes result in a Φ_0-periodic modulation of δG_{rms}, corresponding to a 1.6 T period in $B_{||}$. (**b**) Temperature dependence of the modulation $\delta G_{mod} = \delta G_{rms}^{max} - \delta G_{rms}^{min}$ for all three lengths measured. Dotted lines correspond to the saturation values δG_{mod}^{sat} at low temperatures and solid lines to a power-law behavior at high temperatures. The arrow shows a single crossover temperature $T^* = 1\,K \pm 100\,mK$. (**c**) Longitudinal-field dependence of δG_{rms} for the intermediate length $L_2 = 1\,\mu$m, with $L_2/l_{tr} \gtrapprox 3$, measured at different temperatures. (**d**) Temperature dependence of the amplitude of the standard deviation averaged over $B_{||}$, $\langle \delta G_{rms} \rangle$, and of its maximum peak-to-peak modulation δG_{mod} by a longitudinal field, as inferred from (**c**). Dotted lines correspond to the saturation regimes at low temperatures and solid lines to a power-law behavior at high temperatures. Arrows indicate the different crossover temperatures. Thick line: $1/\sqrt{T}$ dependence of $\delta G_{rms}(T)$ in the regime $L_\varphi(T) < L_2$.

particular[36–38]. The dominant contribution of spin-helical quantized modes to such non-universal conductance fluctuations is unambiguously confirmed by their flux dependence. Indeed, a striking feature is the *periodic modulation* of $\delta G_{rms}(B_{||})$, a hallmark of surface-state transport. All wires show a 1.6 T period in $B_{||}$, which corresponds to a Φ_0 periodicity in flux, in agreement with the electrical cross-section of surface states, taking surface oxidation into account[23]. Remarkably, the amplitude of the modulation is reduced with increasing the length L (Fig. 2a) whereas its damping with temperature does not depend on L (Fig. 2b). Note also that these non-universal conductance fluctuations remain visible even in the longest conductor studied with $L = 6\,\mu$m ($L/l_{tr} \gtrsim 20$), due to quasi-ballistic transport. It could be tempting to relate this behavior to a periodic topological transition due to the perfectly-transmitted mode, as considered in recent studies of Aharonov-Bohm oscillations in 3D TI quantum wires[39–41], but this is not the case here and we show below that non-universal conductance fluctuations result from multi-mode transport and are actually the signature of the weak mixing between spin-helical quantized modes by disorder, due to their spin texture.

The analysis of the temperature dependence of the standard deviation δG_{rms} and of its modulation $\delta G_{mod} = \delta G_{rms}^{max} - \delta G_{rms}^{min}$ by a magnetic flux further reveals two important properties, which are the diffusive nature of the longitudinal motion and the strength of the disorder-induced broadening of quantized transverse modes. We consider the conductor with length $L_2 = 1\,\mu$m ($L/l_{tr} \gtrsim 3$) with more details (see Fig. 2c,d). Since the phase coherence length of helical Dirac fermions is comparable to or longer than the transverse dimension of the nanowire, quantum coherent transport occurs in the quasi-1D limit over the full temperature range studied. At high-enough temperature, $L_\varphi(T) < L$ and the size averaging of conductance fluctuations varies as $\delta G_{rms}(T) \approx \delta G_{rms}^{sat}\left[L_\varphi(T)/L\right]^{\frac{3}{2}}$ (see refs 24 and 29). In the 1D diffusive regime and for decoherence induced by

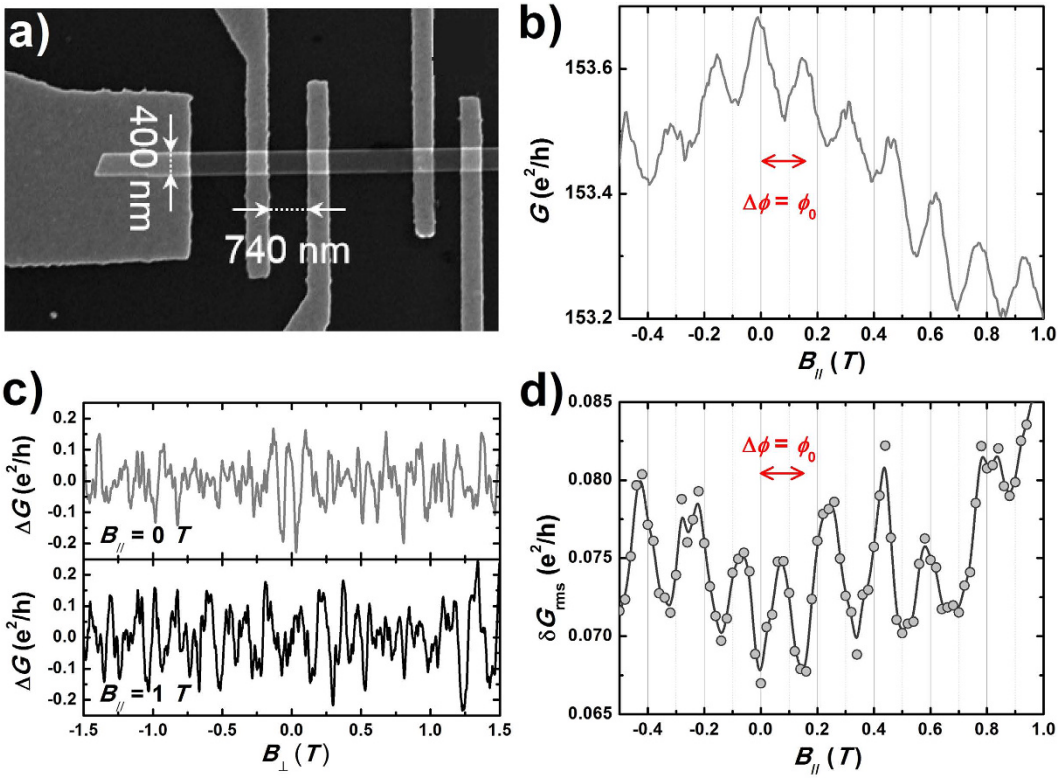

Figure 3. Non-universal conductance fluctuations in a long-perimeter Bi_2Te_3 quantum wire. (**a**) Scanning electron microscope image of a Bi_2Te_3 nanoribbon (width $w = 400$ nm, height $h = 70$ nm and perimeter $L_p = 940$ nm), contacted with CrAu contact pairs with three different lengths $L_1 \approx 740$ nm, $L_2 \approx 1.6\,\mu$m and $L_3 \approx 3.6\,\mu$m. (**b**) Longitudinal magneto-conductance $G(B_{||})$ for the wire with length $L_1 = 740$ nm ($L_1/l_{tr} \gtrsim 1.6$), measured at $T = 100$ mK, showing periodic Aharonov-Bohm oscillations with a 150 mT period. (**c**) Perpendicular magneto-conductance $G(B_\perp)$ at $T = 100$ mK, after the substraction of a slowly-varying background, showing aperiodic conductance fluctuations with a 16 mT correlation field. (**d**) Longitudinal-field dependence of δG_{rms}, inferred from $G(B_\perp)$ traces measured in the ± 1.5 T range. The solid line is the B-spline fit associated to the data points. The modulation corresponds to the expected Aharonov-Bohm Φ_0 flux period, shown as red arrows.

electron-electron interactions[42], $L_\varphi(T) \propto 1/T^{\frac{1}{3}}$ gives $\delta G_{rms}(T) \propto 1/\sqrt{T}$. This reasonably agrees with our measurements for both δG_{rms} and its flux average $\langle \delta G_{rms} \rangle$ (see Fig. 2d), which confirms the different nature of charge transport for the longitudinal and transverse motions in our quantum wires, being diffusive or ballistic, respectively. At very low temperature, δG_{rms} saturates when $L_\varphi(T) \geq L$, a crossover that indeed occurs at $T \approx 200$ mK for the 1 μm long conductor, in agreement with our previous estimations of L_φ inferred from Aharonov-Bohm oscillations[23]. Strikingly, the temperature crossover is much higher for the modulation of δG_{rms} with the longitudinal field. δG_{mod} is temperature independent up to about $T^* = 1$ K, a behavior found for all wire lengths (see Fig. 2b). This shows that the amplitude of non-universal conductance fluctuations is not directly related to L_φ, a result which is not surprising since the flux modulation of δG_{rms} depends on the length even in the fully-coherent regime (as seen in Fig. 2a). This modulation indeed depends on details of the average evolution of quantum states in the reciprocal space, for which the relevant length scale is the transport length, related to the disorder broadening of energy levels. Therefore, the crossover observed at T^* rather corresponds to the limit when the thermal broadening of quantized levels compares to their disorder broadening (see Supplementary Informations: III-C). Thus, this measure gives a direct access to the strength of disorder broadening, and we infer $\Gamma \approx 4 \times k_B T^* \approx 0.4$ meV. This value is much smaller than the energy level spacing $\Delta \approx 6$ meV, so that the mixing of transverse modes by disorder remains limited to a few conductance channels close in energy, an important finding that is confirmed below by theory.

Long-perimeter quantum wires. To confirm the results obtained in a short-perimeter Bi_2Se_3 nanowire, we studied the quantum conductance fluctuations in a wider nanoribbon of another 3D topological insulator Bi_2Te_3 with a perimeter $L_p = 940$ nm (Fig. 3), also grown by vapor transport, for three pairs of CrAu contacts ($L_1 \approx 740$ nm, $L_2 \approx 1.6\,\mu$m and $L_3 \approx 3.6\,\mu$m). The confinement energy $\Delta \approx 1.6$ meV is reduced, and the larger electrical cross section gives a shorter AB period $\Delta B_{||} = 150$ mT. Assuming a Fermi energy $E_F \approx 120$ meV typical for such Bi_2Te_3 nanostructures[41], we obtain an upper bound for the transport length $l_{tr} < 450$ nm from the conductance, so that the condition $L > l_{tr}$ is satisfied for all mesoscopic conductors, and $N \approx 150$ transverse modes. Due to

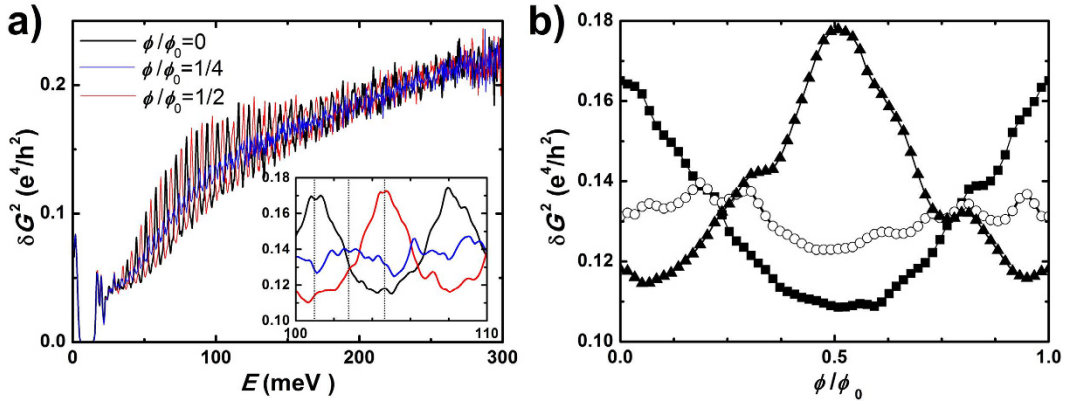

Figure 4. Calculation of the conductance fluctuations in a disordered 3D TI nanostructure. (**a**) Energy dependence of the conductance variance in a disordered 3D topological insulator quantum wire with transverse dimensions similar to the experiment (width $w = 120$ nm, height $h = 20$ nm), a length $L = 350$ nm and a correlation length of disorder of 10 nm, typical of disordered Bi_2Se_3. Calculations are done for a constant transverse field $B_\perp = 1$ T and three different longitudinal fields which correspond to a magnetic flux $\Phi = n\Phi_0$ $\left(n = 0, \frac{1}{4}, \frac{1}{2}\right)$. The inset shows a zoom in a reduced energy window. (**b**) Flux dependence of the conductance variance for three different energies shown as dotted lines in a): $E_0 = 101$ meV (■), $E = E_0 + \frac{1}{4}\Delta$ (○) and $E = E_0 + \frac{1}{2}\Delta$ (▲), with $E_0 \approx E_{(m=14;\Phi/\Phi_0=\frac{1}{2})}$ and $\Delta = 7.2$ meV. When a conductance channel opens, non-universal conductance fluctuations are modulated by the magnetic flux.

the dominant contribution of the fundamental h/e harmonic ($L_\varphi^{SS} \approx L_p$) and to an AB period smaller than the quasi-period of conductance fluctuations due to ($L_\varphi^{BS} < L_p/\pi$), periodic Aharonov-Bohm oscillations are directly visible in the flux dependence of the conductance, as shown in Fig. 3b for the shorter length L_1 (see also Supplem entary Informations: II-A).

Magneto-conductance traces are very different if the magnetic field is applied perpendicularly to the nanoribbon, and reproducible conductance fluctuations are evidenced (see Fig. 3c, for two different values of the magnetic flux $\Phi = B_{||} \times S$). Their correlation field is small ($B_C \approx 16$ mT), so that accurate values of the conductance standard deviation can be extracted from $G(B_\perp)$ traces over a ± 1.5 T range. The Φ_0-periodic modulation of $\delta G_{rms}(B_{||})$ is unambiguously evidenced in Fig. 3d, a result confirmed for the other two longer conductors (see Su pplementary Informations: II-C). As found for Bi_2Se_3 quantum wires, the relative change in δG_{rms} is much larger than the conductance change due to the AB effect. Note also that there is no correlation between the conductance and the amplitude of conductance fluctuations (a thorough analysis in given in Supplementary Informations: II-D), which can be readily seen in Fig. 3b,d), where a minimum of conductance can give either a maximum or a minimum in δG_{rms}. This clear confirmation of non-universal conductance fluctuations due to topological surface states in a Bi_2Te_3 nanoribbon shows that the weak coupling of spin-helical surface modes is a general property of quasi-ballistic 3D topological insulator quantum wires.

Theory

Based on scattering matrix formalism, we show that this unusual behavior in mesoscopic transport results from a combination of both the even energy spectrum of spin-helical Dirac fermions under periodic boundary conditions and their enhanced forward scattering by disorder, due to their spin helicity. To theoretically model our experiments we adapt a continuous Dirac fermion description of the surface state[1,43] and take the bulk as an inert insulator (see Supplementary Information-section III-A). For a fixed chemical potential μ, the number of propagating modes in the nanowire is $N = 2\mu/\Delta$. Since in our experiments N is generally large due to the pinning of the Fermi energy far away from the Dirac point, we studied the evolution of conductance fluctuations over a broad energy range, and our results reveal that the ballistic nature of quantized modes persists in the large-N limit. The statistics of conductance fluctuations is obtained from sampling over many different microscopic configurations of disorder (~1000), and the conductance variance δG_{rms}^2 is calculated for three different values of the flux $\Phi/\Phi_0 = \left(0, \frac{1}{4}, \frac{1}{2}\right)$, which correspond to different configurations of the quantized energy spectrum. For $\Phi/\Phi_0 = \frac{1}{2}$, $E_m = m\Delta$, where m is an integer (mode index). As shown in Fig. 4a) for a fixed perpendicular field $B_\perp = 1$ T, we evidence the energy dependence of the conductance variance, revealing non-universal conductance fluctuations. Close to the charge-neutral Dirac point ($E = 0$), the physics is dominated by a chiral mode arising from quantum Hall physics[7,44,45]. As the energy is increased, quantized transverse modes are weakly perturbed by the transverse field and a clear oscillating behavior of the conductance variance is observed, which corresponds to the opening of discrete transport channels. Since the exact value of the chemical potential at which new channels open depends on the parallel field, these oscillations are shifted by the flux. As a consequence, non-universal conductance fluctuations can be probed at a fixed energy by measuring the flux dependence of the conductance variance. This is shown in Fig. 4b) for three different energies, which correspond to either the opening of a conductance channel ($E = 101$ meV and $E = 104.6$ meV) or to nearly closed or opened channels ($E = 102.8$ meV). The modulation of the variance is indeed periodic in flux, with a period Φ_0, and harmonics are clearly present, as expected in the fully coherent regime. Importantly, the amplitude of the

modulation can be nearly as large as the variance itself, and this is a direct consequence of the limited mixing of quasi-1D modes by disorder. At larger energies, the modulation is reduced due to a larger number of modes (~3–4) contributing to conductance fluctuations, but it remains significant even at $E = 250$ meV, for which both the conductance variance and the amplitude of its modulation compare reasonably well with our experiments.

Discussion

The existence of non-universal conductance fluctuations in a diffusive conductor is at odds with standard theories for massive quasi-particles[27–29] and for Dirac fermions[46,47], which predict universal values of δG_{rms} in the fully-coherent metallic regime ($N \gg 1$). Similar results were found for Dirac fermions in presence of a strong long-range disorder and without quantum confinement, and deviations from a universal value were only found near the ballistic regime[48]. In presence of quantum confinement, although reduced or enhanced conductance fluctuations can occur for a ballistic conductor with a small number of quantized modes[49–53], universality is restored even by a small disorder if the number of transverse modes exceeds a few units[54]. In the long Bi_2Se_3 and Bi_2Te_3 quantum wires studied here, both conditions $L_\varphi > L \geq l_{tr} \gg l_e$ and $G \gg e^2/h$ (number of populated transverse modes $N \gg 1$) should therefore set the system in the universal regime. This is clearly not the case, due to the anisotropic scattering of spin-helical Dirac fermions, and our results suggest that the ballistic nature of quantized transverse modes is robust against disorder, even when approaching the diffusive limit.

In this work, we argue that non-universal conductance fluctuations find their origin in the small broadening Γ of transverse energy levels relative to their energy spacing Δ, as a result of the weak coupling of quasi-1D helical modes by disorder. In general, $\Gamma \gg \Delta$ so that all energy levels overlap. All transverse modes are mixed together by disorder, so that the discretization is washed out and conductance fluctuations are universal. In this limit, there would be no difference between a topological insulator and a charge-accumulation layer at the surface of a semiconductor with strong spin-orbit coupling. This regime corresponds to the case of both metallic and semiconducting nanowires, for which Δ is small and a small disorder induces a rather large broadening Γ of quantized energy levels. In the opposite limit considered here, $\Gamma < \Delta$, a specific transport regime emerges in the crossover between ballistic and diffusive transport, for which signatures of the discreteness and the Dirac nature of the spectrum can be probed even in presence of a large number of modes and close to the diffusive regime for the longitudinal motion. In disordered 3D topological insulator nanostructures, this transport regime is surprisingly robust against a high density of scatterers and it exits over a significantly large energy range. This is due to the weak scattering of spin helical Dirac fermions by disorder, which limits disorder broadening, as well as to the increased energy quantization of Dirac fermions, with respect to massive quasi-particles, and the regular distribution of quantized energies under cyclic boundary conditions. A higher degree of disorder than the one considered here ($l_e \approx 30$ nm) would be required to achieve diffusive transport for high-energy transverse modes. Even in this case, transport would nevertheless remain ballistic close to the Dirac point due to the perfectly-transmitted mode[4]. This situation of *pseudo-ballistic* transport in a diffusive conductor corresponds to the counterpart of *pseudo-diffusive* transport found in ballistic graphene nanostructures at the Dirac point[55–58].

Despite strong disorder, our finding of a weak coupling between quasi-1D helical modes is confirming the potential of 3D TI quantum wires to investigate topological superconductivity. Contrary to the case of semiconducting quantum wires proximitized by a superconducting contact[15], the limited degree of mode mixing could make the detection of a zero-energy Majorana mode by tunnel spectroscopy more difficult but, importantly, novel measurement schemes can be considered[7,21]. Beyond the field of topological superconductivity, our finding also shows that new opportunities in mesoscopic physics can be considered, for instance to investigate the crossover between ballistic and diffusive transport, which was only studied for a relatively weak disorder[59,60] and remains overlooked in a regime of strong disorder. Also, it confirms the possibility to investigate the physics of 3D TI quantum wires with a small number of spin-textured modes, for which a fractional quantization of the conductance and its fluctuations induced by disorder in zero field were predicted[61], as well as the formation of chiral states under a transverse magnetic field[7,61].

Methods

Growth of Bi_2Se_3 and Bi_2Te_3 quantum wires, and Sample preparation. The synthesis of single-crystalline Bi_2Se_3 and Bi_2Te_3 nanostructures was realized by catalyst-free vapor transport in a vacuum sealed silica tube with two compartments separated by a bottleneck[62]. One chamber contains a Bi_2Se_3 or Bi_2Te_3 powder (Sigma-Aldrich) and the other a p^{++}-Si/SiO_x substrate. Electrical properties of wide ribbons were studied in high magnetic fields[32] or using an electrical back gate[31]. Individual nanostructures were imaged with a scanning electron microscope, and their height was measured by atomic force microscopy. For ohmic contacts, a lift-off of CrAuAl or CrAu was made after electron-beam lithography (Zeiss NVision 40), Ar-ion milling and metal deposition (Plassys).

Magneto-transport measurements. Quantum corrections to the conductance of 3D topological insulator quantum wires were measured in a four-probe geometry with lock-in amplifiers, from 4.2 K down to the 20 mK base temperature of a ^{3}He/^{4}He dilution refrigerator (Oxford Kelvinox 300), with a small-enough current polarisation to avoid electronic heating. The base electronic temperature is smaller than 50 mK[23]. Using a three-dimensional vector magnet (Oxford Instruments), the magneto-conductance was investigated with the magnetic field applied either along the nanowire axis, $B_{||}$ up to 6T, or perpendicular to the sample plane, $B_\perp$ up to 2T, with an accuracy of alignement better than 1°.

References

1. Bardarson, J. H., Brouwer, P. W. & Moore, J. E. Aharonov-bohm oscillations in disordered topological insulator nanowires. *Phys. Rev. Lett.* **105,** 156803 (2010).
2. Rosenberg, G., Guo, H.-M. & Franz, M. Wormhole effect in a strong topological insulator. *Phys. Rev. B* **82,** 041104 (2010).

3. Ostrovsky, P. M., Gornyi, I. V. & Mirlin, A. D. Interaction-induced criticality in F_2 topological insulators. *Phys. Rev. Lett.* **105,** 036803 (2010).
4. Bardarson, J. H. & Moore, J. E. Quantum interference and Aharonov-Bohm oscillations in topological insulators. *Reports on Progress in Physics* **76,** 056501 (2013).
5. Cook, A. & Franz, M. Majorana fermions in a topological-insulator nanowire proximity-coupled to an s-wave superconductor. *Phys. Rev. B* **84,** 201105 (2011).
6. Cook, A. M., Vazifeh, M. M. & Franz, M. Stability of majorana fermions in proximity-coupled topological insulator nanowires. *Phys. Rev. B* **86,** 155431 (2012).
7. de Juan, F., Ilan, R. & Bardarson, J. H. Robust transport signatures of topological superconductivity in topological insulator nanowires. *Phys. Rev. Lett.* **113,** 107003 (2014).
8. Alicea, J. New directions in the pursuit of majorana fermions in solid state systems. *Reports on Progress in Physics* **75,** 076501 (2012).
9. Leijnse, M. & Flensberg, K. Introduction to topological superconductivity and majorana fermions. *Semiconductor Science and Technology* **27,** 124003 (2012).
10. Mourik, V. *et al.* Signatures of majorana fermions in hybrid superconductor-semiconductor nanowire devices. *Science* **336,** 1003–1007 (2012).
11. Das, A. *et al.* Zero-bias peaks and splitting in an al-inas nanowire topological superconductor as a signature of majorana fermions. *Nat Phys* **8,** 887, doi: 10.1038/nphys2479 (2012).
12. Churchill, H. O. H. *et al.* Superconductor-nanowire devices from tunneling to the multichannel regime: Zero-bias oscillations and magnetoconductance crossover. *Phys. Rev. B* **87,** 241401 (2013).
13. Bagrets, D. & Altland, A. Class *d* spectral peak in majorana quantum wires. *Phys. Rev. Lett.* **109,** 227005 (2012).
14. Liu, J., Potter, A. C., Law, K. T. & Lee, P. A. Zero-bias peaks in the tunneling conductance of spin-orbit-coupled superconducting wires with and without majorana end-states. *Phys. Rev. Lett.* **109,** 267002 (2012).
15. Pientka, F., Kells, G., Romito, A., Brouwer, P. W. & von Oppen, F. Enhanced zero-bias majorana peak in the differential tunneling conductance of disordered multisubband quantum-wire/superconductor junctions. *Phys. Rev. Lett.* **109,** 227006 (2012).
16. Pikulin, D. I., Dahlhaus, J. P., Wimmer, M., Schomerus, H. & Beenakker, C. W. J. A zero-voltage conductance peak from weak antilocalization in a majorana nanowire. *New Journal of Physics* **14,** 125011 (2012).
17. Lee, E. J. H. *et al.* Zero-bias anomaly in a nanowire quantum dot coupled to superconductors. *Phys. Rev. Lett.* **109,** 186802 (2012).
18. Chang, W., Manucharyan, V. E., Jespersen, T. S., Nygård, J. & Marcus, C. M. Tunneling spectroscopy of quasiparticle bound states in a spinful josephson junction. *Phys. Rev. Lett.* **110,** 217005 (2013).
19. Sau, J. D. & Das Sarma, S. Density of states of disordered topological superconductor-semiconductor hybrid nanowires. *Phys. Rev. B* **88,** 064506 (2013).
20. Takei, S., Fregoso, B. M., Hui, H.-Y., Lobos, A. M. & Das Sarma, S. Soft superconducting gap in semiconductor majorana nanowires. *Phys. Rev. Lett.* **110,** 186803 (2013).
21. Ilan, R., Bardarson, J. H., Sim, H.-S. & Moore, J. E. Detecting perfect transmission in josephson junctions on the surface of three dimensional topological insulators. *New Journal of Physics* **16,** 053007 (2014).
22. Peng, H. *et al.* Aharonov-bohm interference in topological insulator nanoribbons. *Nature Materials* **9,** 225, doi: 10.1038/nmat2609 (2010).
23. Dufouleur, J. *et al.* Quasiballistic transport of dirac fermions in a bi_2se_3 nanowire. *Phys. Rev. Lett.* **110,** 186806 (2013).
24. Akkermans, E. & Montambaux, G. *Mesoscopic Physics of Electrons and Photons* Cambridge University Press (2007).
25. Jalabert, R. A., Baranger, H. U. & Stone, A. D. Conductance fluctuations in the ballistic regime: A probe of quantum chaos? *Phys. Rev. Lett.* **65,** 2442–2445 (1990).
26. Avishai, Y., Touv, J. B., Band, Y. & Kaveh, M. Universal conductance fluctuations in ballistic transport. *Physica A: Statistical Mechanics and its Applications* **168,** 433–438 (1990).
27. Stone, A. D. Magnetoresistance fluctuations in mesoscopic wires and rings. *Phys. Rev. Lett.* **54,** 2692–2695 (1985).
28. Altshuler, B. L. Fluctuations in the extrinsic conductivity of disordered conductors. *JETP Lett.* **41,** 648–561 (1985).
29. Lee, P. A., Stone, A. D. & Fukuyama, H. Universal conductance fluctuations in metals: Effects of finite temperature, interactions, and magnetic field. *Phys. Rev. B* **35,** 1039–1070 (1987).
30. Culcer, D., Hwang, E. H., Stanescu, T. D. & Das Sarma, S. Two-dimensional surface charge transport in topological insulators. *Phys. Rev. B* **82,** 155457 (2010).
31. Dufouleur, J. *et al.* Enhanced Mobility of Spin-Helical Dirac Fermions in Disordered 3D Topological Insulators. *Nano Letters* **16,** 6733–6737 (2016).
32. Veyrat, L. *et al.* Band bending inversion in bi2se3 nanostructures. *Nano Letters* **15,** 7503–7507 (2015).
33. Hsieh, D. *et al.* A tunable topological insulator in the spin helical dirac transport regime. *Nature* **460,** 1101, doi: 10.1038/nature08234 (2009).
34. Kuroda, K. *et al.* Hexagonally deformed fermi surface of the 3d topological insulator Bi_2Se_3. *Phys. Rev. Lett.* **105,** 076802 (2010).
35. Kordyuk, A. A. *et al.* Anomalously enhanced photoemission from the dirac point and other peculiarities in the self-energy of the surface-state quasiparticles in Bi_2Se_3. *Phys. Rev. B* **85,** 075414 (2012).
36. Matsuo, S. *et al.* Weak antilocalization and conductance fluctuation in a submicrometer-sized wire of epitaxial bi_2se_3. *Phys. Rev. B* **85,** 075440 (2012).
37. Lee, J., Park, J., Lee, J.-H., Kim, J. S. & Lee, H.-J. Gate-tuned differentiation of surface-conducting states in $bi_{1.5}sb_{0.5}te_{1.7}se_{1.3}$ topological-insulator thin crystals. *Phys. Rev. B* **86,** 245321 (2012).
38. Choe, D.-H. & Chang, K. J. Universal conductance fluctuation in two-dimensional topological insulators. *Sci. Rep.* **5,** 10997, doi: 10.1038/srep10997 (2015).
39. Hong, S. S., Zhang, Y., Cha, J. J., Qi, X.-L. & Cui, Y. One-dimensional helical transport in topological insulator nanowire interferometers. *Nano Letters* **14,** 2815–2821 (2014).
40. Cho, S. *et al.* Aharonov-bohm oscillations in a quasi-ballistic three-dimensional topological insulator nanowire. *Nat Commun* **6,** 7634, doi: 10.1038/ncomms8634 (2015).
41. Jauregui, L. A., Pettes, M. T., Rokhinson, L. P., Shi, L. & Chen, Y. P. Magnetic field-induced helical mode and topological transitions in a topological insulator nanoribbon. *Nat Nano* **11,** 345, doi: 10.1038/nnano.2015.293 (2016).
42. Altshuler, B. L., Aronov, A. G. & Khmelnitsky, D. E. Effects of electron-electron collisions with small energy transfers on quantum localisation. *Journal of Physics C: Solid State Physics* **15,** 7367 (1982).
43. Bardarson, J. H., Tworzydło, J., Brouwer, P. W. & Beenakker, C. W. J. One-parameter scaling at the dirac point in graphene. *Phys. Rev. Lett.* **99,** 106801 (2007).
44. Lee, D.-H. Surface states of topological insulators: The dirac fermion in curved two-dimensional spaces. *Phys. Rev. Lett.* **103,** 196804 (2009).
45. Ilan, R., de Juan, F. & Moore, J. E. Spin-based mach-zehnder interferometry in topological insulator $p-n$ junctions. *Phys. Rev. Lett.* **115,** 096802 (2015).
46. Kechedzhi, K., Kashuba, O. & Fal'ko, V. I. Quantum kinetic equation and universal conductance fluctuations in graphene. *Phys. Rev. B* **77,** 193403 (2008).
47. Kharitonov, M. Y. & Efetov, K. B. Universal conductance fluctuations in graphene. *Phys. Rev. B* **78,** 033404 (2008).

48. Rossi, E., Bardarson, J. H., Fuhrer, M. S. & Das Sarma, S. Universal conductance fluctuations in dirac materials in the presence of long-range disorder. *Phys. Rev. Lett.* **109,** 096801 (2012).
49. Tamura, H. & Ando, T. Conductance fluctuations in quantum wires. *Phys. Rev. B* **44,** 1792–1800 (1991).
50. Higurashi, H., Iwahuchi, S. & Nagaoka, Y. Conductance fluctuations in mesoscopic quantum wires near the ballistic regime. *Surface Science* **263,** 382–387 (1992).
51. Marcus, C. M., Rimberg, A. J., Westervelt, R. M., Hopkins, P. F. & Gossard, A. C. Conductance fluctuations and chaotic scattering in ballistic microstructures. *Phys. Rev. Lett.* **69,** 506–509 (1992).
52. Nikolić, K. & MacKinnon, A. Conductance and conductance fluctuations of narrow disordered quantum wires. *Phys. Rev. B* **50,** 11008–11017 (1994).
53. Asano, Y. & Bauer, G. E. W. Conductance fluctuations near the ballistic-transport regime. *Phys. Rev. B* **54,** 11602–11611 (1996).
54. Grincwajg, A., Edwards, G. & Ferry, D. Conductance fluctuations in microstructures: Crossover between different transport regimes. *Physica B: Condensed Matter* **218,** 92–96 (1996).
55. Tworzydło, J., Trauzettel, B., Titov, M., Rycerz, A. & Beenakker, C. Sub-poissonian shot noise in graphene. *Phys. Rev. Lett.* **96,** 246802 (2006).
56. Miao, F. *et al.* Phase-coherent transport in graphene quantum billiards. *Science* **317,** 1530–1533 (2007).
57. DiCarlo, L., Williams, J., Zhang, Y., McClure, D. & Marcus, C. Shot noise in graphene. *Phys. Rev. Lett.* **100,** 156801 (2008).
58. Danneau, R. *et al.* Shot noise in ballistic graphene. *Phys. Rev. Lett.* **100,** 196802 (2008).
59. Renard, V. T. *et al.* Quantum corrections to the conductivity and hall coefficient of a two-dimensional electron gas in a dirty *AlGaAs*/*GaAs*/*AlGaAs* quantum well: From the diffusive to the ballistic regime. *Phys. Rev. B* **72,** 075313 (2005).
60. Niimi, Y. *et al.* Quantum coherence at low temperatures in mesoscopic systems: Effect of disorder. *Phys. Rev. B* **81,** 245306 (2010).
61. Zhang, L. *et al.* Universal transport properties of three-dimensional topological insulator nanowires. *Phys. Rev. B* **89,** 245107 (2014).
62. Nowka, C. *et al.* Catalyst-free growth of single crystalline bi2se3 nanostructures for quantum transport studies. *Crystal Growth & Design* **15,** 4272–4278 (2015).

Acknowledgements

J.D. acknowledges the support of the German Research Foundation DFG through the SPP 1666 "Topological Insulators" program. B.D. acknowledges the support of the Alexander von Humboldt Foundation.

Author Contributions

J.D., L.V., B.D. and R.G. fabricated devices, carried out magneto-transport measurements and performed data analysis. C.N. and S.H. synthesized Bi_2Se_3 and Bi_2Te_3 quantum wires. E.X. and J.H.B. performed numerical calculations. B.E. and J.S. helped with the sample preparation. R.G., J.D. and J.H.B. wrote the paper, with contributions from O.G.S. and B.B.

Additional Information

Supplementary information accompanies this paper at http://www.nature.com/srep

Competing Interests: The authors declare no competing financial interests.

How to cite this article: Dufouleur, J. *et al.* Weakly-coupled quasi-1D helical modes in disordered 3D topological insulator quantum wires. *Sci. Rep.* **7**, 45276; doi: 10.1038/srep45276 (2017).

Publisher's note: Springer Nature remains neutral with regard to jurisdictional claims in published maps and institutional affiliations.